

Quantum phase transition from a Antiferromagnetic-Insulator to a Paramagnetic-Metal laying beneath the superconducting dome

Victor M. Martinez Alvarez^{*,***}, Alejandro Cabo-Bizet^{**} and Alejandro Cabo^{*}

^{*} *Department de Física Teórica, Instituto de Cibernética, Matemática y Física, Calle E, No. 309, Vedado, La Habana, Cuba.*

^{**} *Department de Física, Centro de Aplicaciones Tecnológicas y Desarrollo Nuclear, Calle 30, No. 502 e/ 5ta y 7ma Avenida, Playa, La Habana, Cuba. and*

^{***} *Department de Física, Universidad de Camagüey, Circunvalación Norte, km 5, Camagüey, Cuba.*

The effect of hole doping on the Tight-Binding (*TB*) model of the *Cu-O* planes in the *La₂CuO₄* constructed in previous works is investigated here. Firstly, it is pointed out that the model employed constitutes a generalization of the Hubbard one for the same system. Thus, the former predictions of the insulator gap, antiferromagnetic (*AF*) character and the existence of a paramagnetic-pseudogap (*PPG*) state at half-filling, become natural ones to be expected from this more general picture. The effect of hole doping on the antiferromagnetic-insulator state (*AFI*) and the paramagnetic-pseudogap one at half-filling, is investigated here at $T = 0 K$. The results predict the occurrence of a quantum phase transition (*QPT*) from the antiferromagnetic-insulator state at low doping to a paramagnetic-metallic state (*PM*) at higher hole densities. Therefore, a clear description of the hidden *QPT* laying beneath the “dome” in high critical temperature (*HT_c*) superconducting materials is found. At low doping, the systems prefers the *AFI* state, and at the critical value of the doping density $\delta_c = 0.2$, the energy of a metallic state starts becoming lower. The evolution with small doping values of the band spectrum of the *AFI* state, shows that the holes tend to become localized at the middle of the sides of the reduced Brillouin zone (*BZ*). Then, when δ passes through the critical value, the holes of the *AFI* state move to become situated at the corners of the same reduced *BZ*, showing in this way a structural change at the phase transition point. Thus, the *PM* state which appears at the transition point acquires the same behavior with respect to the localization of holes as the pseudogap state. In the small doping limit a clear difference between the degree of convergence of the iterative self-consistent solution is associated to an even or odd number of electrons. It suggests that the Kramers degeneration in combination with the spin-spatial entangled nature of the hole states, leads to a new kind of pair interaction between two holes. The binding energy value is estimated as a function of the screening.

PACS numbers: 71.10.-w,74.72.-h,74.72.Gh,74.72.Kf,75.10.-b,71.30.+h

I. INTRODUCTION

Since the discovery of the high critical temperature superconductivity in the called “cuprates” (made up of copper oxides) [1], the search about the nature of their behavior has been and it continues being, one of the most defiant and investigated topics in Condensed Matter Physics. Among these compounds is the *La₂CuO₄*, that is a classic example of the so-called strongly correlated electron systems (*SCES*). However, due to the inherent difficulties of the many body problem for this class of materials, numerous properties continue without being clearing up, in spite of the efforts done by the investigators in this subject. The *La₂CuO₄* superconductor is characterized by a drastic change in its behavior depending on the density of electrons in the two-dimensional planes *CuO₂* [2], and it happens in general in the *HT_c* superconductivity materials. All the cuprate superconductors have as a common element, the existence in their crystal structure of *CuO₂* planes.

The standard band calculations predict a character of paramagnetic-conductor to this material [3], in drastic contrast with its experimentally observed, insulating and antiferromagnetic nature. These two properties are associated with the presence of strong correlations, and are not derivable starting from an independent particle scheme as the Hartree-Fock (*HF*) one, when the whole many electron crystal system is considered [2]. However, in Refs. [4–6], on the base of a single band model solved in the *HF* approximation, it was possible to predict the mentioned *SCES* properties of this material. At first sight, it might seem that to obtain the *AF* and insulating properties of *La₂CuO₄* from a *HF* scheme, could be a contradictory outcome, since those properties are thought as essentially indicating the strong correlation nature of this material. However, those results become natural ones, when considering the following circumstances. In first place, the *HF* procedure was not applied in its quality of a *First Principle* method to solve the full Hamiltonian problem associated to the total electronic structure of *La₂CuO₄*. Alternatively, the procedure was employed for solving the simple model of the *CuO₂* layers built in Refs. [4–6]. It is well-known that the impossibility of describing strong correlation properties by employing the *HF* scheme, appears when the scheme is applied to find the solution of the exact many electron problem defined by all the electrons and nuclei constituting a crystalline solid. For example, the

direct *HF* calculation of the band structure of La_2CuO_4 , predicts an enormous electronic gap of nearly of 17 eV [7]. In addition, the model introduced in Refs. [4–6], only considers the electrons that half-filled the single band crossing the Fermi level appearing in the early electronic band calculation [3]. In fact, the proposed simple Hamiltonian can be viewed as a preliminary stage within the definition of one among the variety of Hubbard’s Hamiltonians. One, in which the last step of imposing the nearest neighbor approximations leading to the Hubbard theories had not been implemented. Therefore, the proposed model could be considered as an improvement of a Hubbard one, which retains the full Coulomb repulsion operator intact [8]. This last point can be understood by keeping in mind that its free Hamiltonian is basically a *TB* one in which the full Coulomb interaction operator between the electrons had been retained. Thus, after performing the nearest neighbor approximations, a typical Hubbard scheme arises. Henceforth, since the Hubbard model is recognized to convey strong correlation effects, and moreover, since it is also known that its mean field solutions also can exhibit such effects [8], the appearance of the insulator gap and the antiferromagnetic structure in Refs. [4–6], becomes a reasonable conclusion. However, a new physical prediction coming from the analysis is the existence of pseudogap states, which are not following in the Hubbard approximation. These mentioned results emerged as a consequence of a combination of lattice symmetry breaking with a spin-space entanglement structure in the single particle solutions of the *HF* problem. The treatment gave a clear explanation about the nature of the antiferromagnetism and the insulating structure of this high temperature superconductor.

The process through which the electronic structure evolves with the hole doping, from the *AFI* state at low doping to the superconductor state, and then to a normal metal phase at large hole concentrations, has been the subject of a strong interest in the literature. It is known that the magnitude of the gap in the normal state is of the same order that the superconductor gap [9]. With the objective of studying the hole doping dependence of the band structure, the $La_{2-x}Sr_xCuO_4$ (*LSCO*) system is for several reasons appropriate among the family of the *HTc* superconductors. In first place, the *LSCO* has a simple crystalline structure of CuO_2 layers. Second, the concentration of holes in these planes can be controlled in a wide range and is uniquely determined by the concentration x of *Sr* [9]. For this reason, one can develop samples of the material by varying doping continuously from the insulating state without doping ($x = 0$) up to the high doping limit ($x = 0.3$) in the same system.

Numerous experiments made in copper oxide compounds, suggest the existence of a quantum phase transition at $T = 0\text{ K}$, which lays inside the doping interval of the superconducting dome (this is colloquially referred as “laying beneath” the dome). It is believed that this *QPT* is the key to understand the high temperature superconductivity and also to explain the properties of the normal state in those materials [10, 11]. The present work presents results that predict the existence of this sort of *QPT* in the context of the model for the La_2CuO_4 constructed in Refs. [4–6] when the hole doping is incorporated. The *HF* system of equations is solved here by employing the same method used in Refs. [4–6]. In the present case, again the parameters of the model are determined of imposing the condition that the *HF* solution without crystalline symmetry breaking, reproduces the form of the single band crossing the Fermi level in the band calculations of the material [3]. Then, we investigated the changes that occur in the band structure when the system is doped with holes. As in Refs. [4–6] at exact half-filling, the *HF* solution predicts the existence of the *AFI* and *PPG* states. This previous result motivated the idea of investigating the hole doping consequences, after conceiving the possibility of predicting the quantum phase transition at $T = 0\text{ K}$. The same existence of this transition, is currently one of the most fundamental questions in high temperature superconductivity research [10, 11]. A transition like this is now considered that should determine the properties of the normal state in the diverse regions of the phase diagram. The present investigation aim consists in studying the existence of this quantum phase transition beneath the superconducting dome.

The Hartree-Fock description of the simple model for the $Cu-O$ planes of La_2CuO_4 including symmetry breaking effects and spin-spatial “entanglement” of the single particle states at half-filling, is here extended to consider the effects of hole doping. It is observed how the effect of doping is able to predict a variety of the most interesting properties of this material a $T = 0\text{ K}$. The evolution of the band spectrum of the antiferromagnetic-insulator and the paramagnetic-pseudogap states as functions of the hole doping parameter are determined, for a wide range of the hole concentration $0 \leq x \leq 0.3$. Around the critical doping $x_c = 0.2$, the results show that for the *AFI* state, the band spectrum suffers a gradual change, in which the insulator gap diminishes to completely closing. Surprisingly, the same behavior occurs for the *PPG* state for which the pseudogap also collapses. For higher values than the mentioned critical doping one, the *AFI* and *PPG* states coalesce in a single *HF* solution. The magnetization of this high doping state vanishes as well as its gap, thus, it describes a paramagnetic-metallic phase. The results also reveal a drastic change in the Fermi surface, which goes from a hole-like Fermi surface centered at (π, π) for $0 < x < 0.2$ into an electron-like one centered at $(0, 0)$ for $0.2 < x \leq 0.3$. These results evidence the existence of a quantum phase transition laying beneath the superconductor dome, in which an insulator state with antiferromagnetic correlations transits to a paramagnetic-metallic phase. The work also identifies a new mechanism of hole pairing which could give rise to the superconductivity. The effect results from a combination of the Kramers degeneration with the spin-spatial entanglement of the single particle *HF* states. The discussion helps to clarify the relation between: the pair of states *AFI* and *PPG* in the Physics of the strongly correlated electron systems with the superconductor state and the

quantum critical point, around which the phase transition occurs [10–13]. An evaluation of the hole pairs binding energy as a function of the dielectric constant is obtained, which predicts binding of the pairs at the experimentally measured values of the dielectric constant of La_2CuO_4 [14]. However, the thermodynamic limit for this calculation had not been attained yet in this work. In addition, the parameters of the model should be optimized yet to match the measured parameters of the material as the insulator gap of 2 eV [15], and the dielectric constant having a value of the order of 25 [14]. Here, it is pointed out that this binding effect could be the acting mechanism determining the physical relevance of the doubly charged bosonic fields argued in Ref. [16].

The paper is organized as follows. In section 2 we review the one band model of the $Cu-O$ planes in La_2CuO_4 introduced in Refs. [4–6], the procedure for the determination of its parameters and the Hartree-Fock solution for the here considered situation: the study of the hole doping effects. In section 3 the results are presented for the evolution of the band spectrum of the PPG state in the range of doping $0 \leq x \leq 0.3$. Next, the section 4 considers the same study for the AFI state. Section 5 presents the results for the changes of the Fermi surfaces as the doping is increased. The quantum phase transition properties are discussed in section 6. At the section 7 we expose the identification of a possible hole pairing mechanisms which could give rise to the superconductivity and estimate the values of the energy for pair binding. Finally, the conclusion are presented in section 8.

II. THE CuO_2 MODEL INCLUDING HOLE DOPING

In this section we will review the main ideas and elements defining the model for the La_2CuO_4 introduced in Refs. [4–6]. In the first subsection, the structure and notation of the unrestricted Hartree-Fock scheme employed is described. Next, the model is presented.

A. Fully unrestricted Hartree-Fock scheme

The N electron system considered in the TB model discussed in Refs. [4–6] was described by a fully unrestricted Slater determinant $f_n(x_1; s_1, \dots, x_N; s_N)$ state constructed with single particle orbitals $\phi_{k_i}(x_i, s_i)$ with $i = 1, \dots, N$, which arbitrarily depends on the spin variables at any point of the space. The index n represents the set of quantum numbers of the many electron system. In this subsection, as usual, generalized coordinates will be assumed to incorporate the spatial in common with the spin ones. For the electron case under study, the Slater determinant gets the expression

$$f(x_1; s_1, \dots, x_N; s_N) = \frac{1}{\sqrt{N!}} \sum_{\eta_1, \dots, \eta_N} \epsilon^{\eta_1, \dots, \eta_N} \phi_{\eta_1}(x_1, s_1) \dots \phi_{\eta_N}(x_N, s_N), \quad (1)$$

$$\forall_i \eta_i = k_1, \dots, k_N,$$

where $\epsilon^{\eta_1, \dots, \eta_N}$ is the Levi-Civita tensor. The single particle HF orbitals satisfy a set of coupled integro-differential equations of the Pauli kind. This set is derived from the minimization of the HF energy functional of the system under the conditions of normalization of f and the normalization of all the single particle orbitals ϕ_{k_i} . For more details see Refs. [4–6]. In general, the Hamiltonian of usual electronic systems has a free term $\sum_i \hat{\mathcal{H}}_0(x_i)$ (a kinetic energy plus an interaction with an external field one) with an addition associated to the pair Coulomb interaction between the electrons in the form

$$\hat{\mathcal{H}}(x_1, \dots, x_N) = \sum_i \hat{\mathcal{H}}_0(x_i) + \frac{1}{2} \sum_{j \neq i} V(x_i, x_j). \quad (2)$$

After performing the above referred minimization process by using the Lagrange multipliers scheme, a “fully unrestricted” set of HF equations for the orbitals ϕ_{k_i} is obtained in the form

$$[\hat{\mathcal{H}}_0(x) + \sum_{\eta_1} \sum_{s'} \int d^2x' \phi_{\eta_1}^*(x', s') V(x, x') \phi_{\eta_1}(x', s')] \phi_{\eta}(x, s) -$$

$$\sum_{\eta_1} [\sum_{s'} \int d^2x' \phi_{\eta_1}^*(x', s') V(x, x') \phi_{\eta}(x', s')] \phi_{\eta_1}(x, s) = \varepsilon_{\eta} \phi_{\eta}(x, s), \quad (3)$$

where $\eta, \eta_1 = k_1, \dots, k_N$. In this completely unrestricted way, the HF set of equations was wrote by Dirac [17]. In this form, the orbitals are allowed to show arbitrary spin projection at any point of the space, and this determines the use

of the terms “fully unrestricted” for this set of equations. The total HF energy of the N electron system E_{HF} and the HF single particle energies have the forms

$$\begin{aligned} E_{HF} &= \sum_{\eta} \langle \eta | \hat{\mathcal{H}}_0 | \eta \rangle + \frac{1}{2} \sum_{\eta, \eta_1} \langle \eta, \eta_1 | V | \eta_1, \eta \rangle - \frac{1}{2} \sum_{\eta, \eta_1} \langle \eta, \eta_1 | V | \eta, \eta_1 \rangle, \\ \varepsilon_{\eta} &= \langle \eta | \hat{\mathcal{H}}_0 | \eta \rangle + \sum_{\eta_1} \langle \eta, \eta_1 | V | \eta_1, \eta \rangle - \sum_{\eta_1} \langle \eta, \eta_1 | V | \eta, \eta_1 \rangle. \end{aligned} \quad (4)$$

The definitions of the basis states of the one electron band model and their scalar products appearing in the above equations are specified in Refs. [4–6].

1. The α and β spin constraints.

The analysis in Refs. [4–6] was initially motivated by the aim of examining the restrictions that could be introduced in the description of many particle systems, by the frequently employed assumption about that the HF single particle states should have a definite $+1/2$ (α) or $-1/2$ (β) projection of their spin at all the spatial points. That is, to show the structure:

$$\phi_k(x, s) = \begin{cases} \phi_k^{\alpha}(x) u_{\uparrow}(s) & \text{type } \alpha, \\ \phi_k^{\beta}(x) u_{\downarrow}(s) & \text{type } \beta. \end{cases} \quad (5)$$

Whenever the spatial functions $\phi_k^{\alpha}(x)$ are identical, the HF evaluation is called a *restricted* one, and when they can be different it is described as an *unrestricted* one [18]. However, both of these cases are in fact restrictive ones for the allowed spin orientations of the HF orbitals. It was emphasized in references [4–6] that these assumptions about the spin structure of the orbitals can be characterized as definite constraints which drastically limits the generality of the space of function in which the HF single particle orbitals are searched. It can be noted that the HF scheme introduced by Dirac [17] does not include any restriction on the spin structure of the searched orbitals.

B. The model for the CuO_2 planes

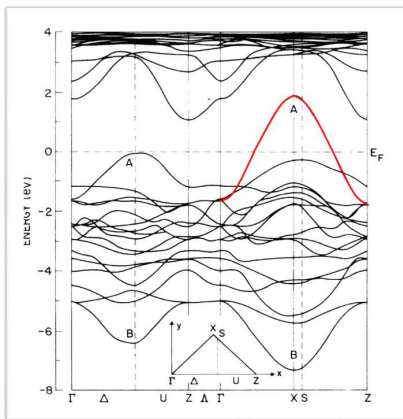


FIG. 1: Band structure of the La_2CuO_4 , calculated by Matheiss 1987. The single half-filled band suggests the consideration of the here investigated model, which is based in a set of interacting electrons subject to a crystalline TB potential, tightly binding them to the points of the lattice formed by the Cu atoms in the material.

In figure 1, a calculated band diagram of the La_2CuO_4 is illustrated. The band structure was obtained by the use of the $LAPW$ (Linear Augmented Plane Waves) method [3]. Let us describe below the formulation of the model for the CuO_2 planes introduced in Refs. [4–6], which is the starting point of the present work. It can be noted that the last band occupied by electrons is half-filled, a fact that indicates a metallic character for the material. The form of this band suggested the validity of an approximate TB description for the electrons populating it. The less bound kind of electron in the compound La_2CuO_4 , is the unpaired one in the Cu^{2+} , which at variance with the O^{2-} in the plane, does not has its last shell ($3d$) closed. These electrons, in a qualitative picture can be estimated to be the ones

constituting the mentioned unique band crossing the Fermi level in the band calculations done in the Ref. [3]. These electrons can be reasonably considered as tightly bound to the *Cu* atoms in the *CuO₂* planes, assumed the completion of the *O²⁻* atoms in those planes. The last remarks, support the idea of taking as the lattice defining the *TB* model, that one giving rise to the half-filled band in Ref. [3]. That is, the planar squared lattice of points coinciding with the sites of the *Cu* atoms in the *CuO₂* plane (see figure 2).

The presence of all the other electrons filling the rest of the bands, in common with all the neutralizing nuclear charges, were taken to play a double role in the model defined in Refs. [4–6]. In one sense, this system is assumed as a polarizable effective medium which screens the Coulomb repulsion by means of effective dielectric constant ϵ . In second place, this system is assumed to generate a mean periodic Tight Binding potential W_γ , which strongly confines the electrons of the single partially filled band to be close to the *Cu* atoms in the *CuO₂* planes. The model is assumed to be purely *2D*, that is, the space coordinates are assumed to have only two planar components $\mathbf{x} = (x_1, x_2)$. It is completed by assuming that the electrons in the partially filled band are also interacting with the potential F_b generated by a jellium charge density which neutralizes the net charge of the electrons of the model. The jellium charges were assumed as periodically concentrated and having a planar gaussian distribution with a radial width defined by the parameter b . In resume, the free Hamiltonian for the *TB* model for the electrons in the half-filled band has the form

$$\hat{H}_0(\mathbf{x}) = \frac{\mathbf{p}^2}{2m} + W_\gamma(\mathbf{x}) + F_b(\mathbf{x}), \quad (6)$$

in which the periodic *TB* potential is satisfying the periodicity condition

$$W_\gamma(\mathbf{x}) = W_\gamma(\mathbf{x} + \mathbf{R}), \quad (7)$$

and the jellium potential is defined by

$$F_b(\mathbf{x}) = \frac{e^2}{4\pi\epsilon_0\epsilon} \sum_{\mathbf{R}} \int d^2y \frac{\exp(-\frac{(\mathbf{y}-\mathbf{R})^2}{b^2})/\pi b^2}{|\mathbf{x}-\mathbf{y}|}, \quad b \ll p, \quad (8)$$

in which the coordinate vectors of the planar *Cu* atoms are

$$\mathbf{R} = n_{x_1}p \mathbf{e}_{x_1} + n_{x_2}p \mathbf{e}_{x_2} \quad \text{where} \quad n_{x_1}, n_{x_2} \in \mathbb{Z}, \quad (9)$$

where the unit vectors \mathbf{e}_{x_1} and \mathbf{e}_{x_2} lay on directions defined by the vectors joining the nearest neighbors of the *Cu* atoms in the lattice in figure 2. It is known that the distance between a *Cu* atoms and its nearest neighbor is $p = 3.82 \text{ \AA}$ [19]. Further, the Coulomb interaction between two electrons in the partially filled band of the model is assumed in the form

$$V = \frac{e^2}{4\pi\epsilon_0\epsilon} \frac{1}{|\mathbf{x}-\mathbf{y}|}, \quad (10)$$

including a dielectric constant which is supposed to be generated by the polarization of the set of electrons filling the other bands and all the nuclei in the *La₂CuO₄*, through which the electrons of the partially filled band of the model are assumed to move.

The model was started to be constructed with the initial idea of searching for *HF* single particle states of the electrons in the partially filled band, not being of an α or β types, that is, not being separable in their spatial and spin dependence. In other words, allowing that in those *HF* orbitals the spin projection could depend on the spatial position (spin-space entanglement or non collinear spin structure). Materials showing *AF* structure were suspected to lead to *HF* solutions of this kind, a fact that also suggested the possibility of improving the understanding of the troublesome state of knowledge of the band structure of such materials. In the particular case of the *La₂CuO₄*, it is known that it is an antiferromagnetic compound. In the *AF* systems, normally the crystal symmetry of the substance is directly broken by the *AF* order. Therefore the description of the model was also designed to incorporate the possibility of the breaking of the crystalline translation invariance. The *AF* order has translation symmetry in each one of the two interpenetrating squared sublattices in which the planar *Cu* lattices can be decomposed. Thus, the *HF* single particle orbitals in the model were assumed to retain the Bloch functions character under the common reduced translation symmetry group of these sublattices. Then, the physical state should be equivalent under the translations leaving invariant the sublattices, but not under the one which transforms a sublattice into the other. This reduced symmetry is associated to a subgroup of the total translation group of the crystal and therefore its space representation should be more reduced in its number of states as classified by the momenta \mathbf{k} in the reciprocal space.

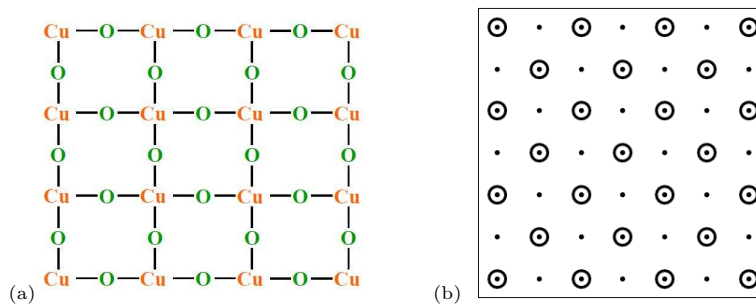


FIG. 2: (a) The picture illustrates the CuO_2 planes in the material. (b) Point lattice associated to those planes. In the search of the possibility of describing the AF properties of the material through the elimination of the symmetry restrictions (over the space of functions in which the single particle states were searched) it was helpful to decompose the full lattice in the two sublattices which are differentiated in the picture.

The two sublattices of point depicted in figure 2, that will be described below by the indices $r = 1$ or 2 , are analytically defined in the form

$$\mathbf{R}^{(r)} = \sqrt{2}n_1p \mathbf{q}_1 + \sqrt{2}n_2p \mathbf{q}_2 + \mathbf{q}^{(r)}, \quad (11)$$

$$\mathbf{q}^{(r)} = \begin{cases} \mathbf{0} & \text{if } r = 1 \\ p \mathbf{e}_{x_1} & \text{if } r = 2, \end{cases}$$

where \mathbf{q}_1 and \mathbf{q}_2 are the two unit vectors defining the directions of the unit cell vector of the sublattices.

1. Sublattice translations

Then, the searched HF single particle wave functions should be eigenfunctions of the discrete translation operator $\hat{T}_{\mathbf{R}^{(1)}}$, which transform a sublattice in itself

$$\hat{T}_{\mathbf{R}^{(1)}} \phi_{\mathbf{k},l} = \exp(i\mathbf{k} \cdot \mathbf{R}^{(1)}) \phi_{\mathbf{k},l}. \quad (12)$$

When the point lattice is infinite, the Brillouin cell formed by the set of all the momenta \mathbf{k} indexing the eigenfunctions of $\hat{T}_{\mathbf{R}^{(1)}}$ is the shadowed zone in figure 3, while the large square represents the set of momenta associated to the eigenfunctions of the group of translations in the original lattice. Since it is impossible to numerically treat the infinite lattices because it has a continuum of states, periodical boundary conditions were chosen in order to make finite the number of eigenfunctions in the Brillouin zone. The boundary conditions were imposed fixing the periodicity of the eigenfunctions $\phi_{\mathbf{k},l}$ in the boundaries defined by $x_1 = -Lp$ and $x_1 = Lp$ along the x_1 axis and by $x_2 = -Lp$ and $x_2 = Lp$ along the x_2 axis. The finite set of momenta vectors obeying the boundary conditions are

$$\mathbf{k} = \begin{cases} \frac{2\pi}{Lp}(n_{x_1} \mathbf{e}_{x_1} + n_{x_2} \mathbf{e}_{x_2}) \\ n_{x_1}, n_{x_2} \in \mathbb{Z} \\ -\frac{L}{2} \leq n_{x_1} \pm n_{x_2} < \frac{L}{2}. \end{cases}$$

The number of electron eigenfunctions obeying the conditions is $\frac{N}{2}$, that is, a half of the number of functions satisfying the same boundary periodicity conditions when the group is the group of translations in the full point lattice.

2. Tight-Binding single band basis

The TB basis that was employed for describing the one band model had the form

$$\varphi_{\mathbf{k}}^{(r,\sigma_z)}(\mathbf{x}, s) = \sqrt{\frac{2}{N}} u^{\sigma_z}(s) \sum_{\mathbf{R}^{(r)}} \exp(i\mathbf{k} \cdot \mathbf{R}^{(r)}) \varphi_0(\mathbf{x} - \mathbf{R}^{(r)}), \quad (13)$$

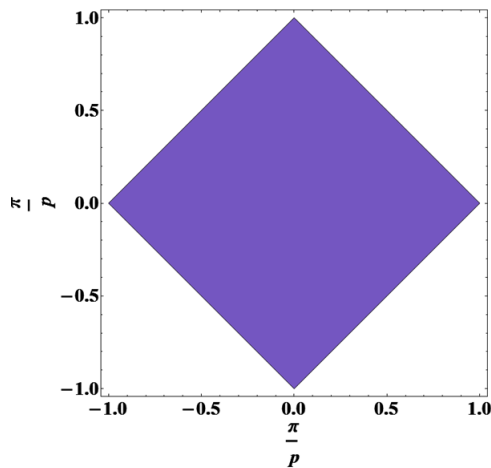


FIG. 3: The darker region shows the reduced Brillouin zone associated to the Bloch functions defined on the sublattices. The length of its sides is $\sqrt{2}\frac{\pi}{p}$.

$$\hat{\sigma}_z u^{\sigma_z} = \sigma_z u^{\sigma_z},$$

$$\varphi_0(\mathbf{x}) = \frac{1}{\sqrt{\pi a^2}} \exp\left(-\frac{\mathbf{x}^2}{2a^2}\right), \quad a \ll p. \quad (14)$$

where N is the number of electrons in the model electron gas filling part of the band crossing the Fermi level and $\hat{\sigma}_z$ is the spin projection operator in the z axis, which is assumed to be orthogonal to the CuO_2 planes; $\sigma_z = -1, 1$ are its eigenvalues; $r = 1$ and 2 , is the above defined index for each of the two sublattices. Note that in the small overlapping approximation between nearest neighborhood points (which should be in different sublattices), the orthogonality between the members of this basis is only lost between functions belonging to different sublattices having the same spin polarization and momentum. The orthogonality between distinct elements corresponding to the same sublattice is valid by construction.

The chosen Wannier orbital of the model $\varphi_0(\mathbf{x} - \mathbf{R}^{(r)})$ were fixed for simplicity. Their gaussian form implies that it was supposed that the net TB potential in the close neighborhood of each Cu atom had been assumed to be a simple 2D harmonic potential. This simplifying assumption was adopted following the idea that the main forces in defining the AF and insulator properties of the CuO_2 planes were in fact determined by the spontaneous breaking of the crystalline symmetry plus the spin entangled structure of the HF electron orbitals. Thus, simplifying considerations led to fix the explicit form of equation (13) for the starting basis states of the model. However, taking into account improved definitions for the Wannier's orbitals defining the single band model, might be of help for the description of other effects, by example the magnetic anisotropy of the AF order in La_2CuO_4 . For this purpose, the model could be generalized by considering atomic $3D$ representation, employing Wannier's orbitals like the d ones of the Cu and the inclusion of spin-orbit interactions. This study is expected to be considered elsewhere.

C. Hartree-Fock solution with hole doping

In this subsection we present the matrix problem to which the HF set of equations of the model was reduced in Refs. [4–6], after its projection on the defined basis. In the present work, these equations will be solved for the more general situation in which the system is doped with holes. In the coming subsection it will be reviewed how the model reproduces the main characteristics of the dispersion of the single band crossing the Fermi level in Ref. [3] (predicting a metallic and paramagnetic state) when full crystalline symmetry and the HF orbitals of the type α and β are assumed. Afterwards, the next sections will illustrate the consequences of the elimination of the symmetry restrictions in the space of functions in which the HF energy functional is minimized. It was performed in a similar way as it was done in Refs. [4–6], but for the important situation in which the systems is doped with holes. At very small doping values, the solutions are the ones obtained in Refs. [4–6] for the exact half-filling situation: the ground state is an antiferromagnetic-insulator and the excited phase corresponds to the paramagnetic-pseudogap state. When the hole doping is augmented the results indicate the appearance of a quantum phase transition at the doping value $x = 0.2$, in which the AFI and PPG states both coalesce in one single metallic state for higher doping values.

As in Refs. [4–6] the searched HF single particle states are expressed as a linear combination of the before defined basis functions in the form

$$\phi_{\mathbf{k},l}(\mathbf{x}, s) = \sum_{r,\sigma_z} B_{r,\sigma_z}^{\mathbf{k},l} \varphi_{\mathbf{k}}^{(r,\sigma_z)}(\mathbf{x}, s), \quad (15)$$

where l is the index of the quantum numbers required to uniquely define the HF single particle states. After substituting the above expression for the orbitals in the HF equations and taking their scalar product with an arbitrary state, the equivalent self-consistent matrix problem can be written in the form

$$[E_{\mathbf{k}}^0 + \tilde{\chi}(G_{\mathbf{k}}^{Co} - G_{\mathbf{k}}^{int} - F_{\mathbf{k}})] \cdot B^{\mathbf{k},l} = \tilde{\varepsilon}_l(\mathbf{k}) I_{\mathbf{k}} \cdot B^{\mathbf{k},l}, \quad (16)$$

with the definitions for the constants

$$\tilde{\chi} = \frac{me^2 a^2}{4\pi \hbar^2 \epsilon \epsilon_0 p}, \quad (17)$$

$$\tilde{\varepsilon}_l(\mathbf{k}) = \frac{ma^2}{\hbar^2} \varepsilon_l(\mathbf{k}), \quad (18)$$

which are dimensionless, as also are all the implicit parameters in the definitions of all the entering matrices

$$E_{\mathbf{k}}^0 = \left\| E_{\mathbf{k},(t,r,\alpha_z,\sigma_z)}^0 \right\|_{4 \times 4},$$

$$G_{\mathbf{k}}^C = \left\| G_{\mathbf{k},(t,r,\alpha_z,\sigma_z)}^C \right\|_{4 \times 4},$$

$$G_{\mathbf{k}}^i = \left\| G_{\mathbf{k},(t,r,\alpha_z,\sigma_z)}^i \right\|_{4 \times 4},$$

$$F_{\mathbf{k}} = \left\| F_{\mathbf{k},(t,r,\alpha_z,\sigma_z)} \right\|_{4 \times 4},$$

$$I_{\mathbf{k}} = \left\| I_{\mathbf{k},(t,r,\alpha_z,\sigma_z)} \right\|_{4 \times 4}.$$

They are respectively associated to the kinetic term plus the periodic TB potential, the Coulomb direct and exchange potential terms, the potential generated by the compensating jellium charge density and the overlapping matrix between the basis functions. The formulae for the matrix elements are shown in the Appendices of the Refs. [5, 6]. In the employed representation the normalization condition of the HF single particle states and the formula for the HF energy take the forms

$$1 = B^{\mathbf{k},l*} \cdot I_{\mathbf{k}} \cdot B^{\mathbf{k},l}, \quad (19)$$

$$E_{\mathbf{k},l}^{HF} = \sum_{\mathbf{k},l} \Theta_{(\tilde{\varepsilon}_F - \tilde{\varepsilon}_l(\mathbf{k}))} [\tilde{\varepsilon}_l(\mathbf{k}) - \frac{\tilde{\chi}}{2} B^{\mathbf{k},l*} \cdot (G_{\mathbf{k}}^C - G_{\mathbf{k}}^i) \cdot B^{\mathbf{k},l}]. \quad (20)$$

The HF matrix system of equations (16) is a non linear one in the variables $B_{r,\sigma_z}^{\mathbf{k},l}$, which are the four components of the vector $B^{\mathbf{k},l}$ for each value of \mathbf{k} . The B constants can be interpreted as determining the probability amplitudes to find the electron in the states (\mathbf{k}, l) , of the sublattice r , and spin along the z axis. Note that for each \mathbf{k} value, four values of the quantum numbers of the HF single particle states $l = 1, 2, 3, 4$ should be obtained, or what is equivalent, four bands in the reduced BZ . From the equations (16) it can be observed that the full matrix representation of the Fock operator is block diagonal in the momenta indices \mathbf{k} , which is a direct consequence of the symmetry with respect to the reduced translation invariance of the system.

D. Maximal symmetry solutions: fixing the model parameters

In first place the HF problem was solved by assuming that the HF single particle states satisfied the translation invariance in the whole lattice and also were showing α or β spin dependence. After this assumptions, as it was suspected, the HF solution of the model produced the single particle spectrum depicted in the figure 4, in a similar way as in Refs. [4–6]. As before we will adjust the free parameters ϵ : the dielectric constant of the effective medium; \tilde{a} : the radial distance for which the gaussian Wannier's orbitals are appreciably different from zero; $\tilde{\gamma}$: the hopping probability between nearest neighbor sites fixed by the effective medium and \tilde{b} : radial distances inside which the jellium charges are concentrated.

The Bloch Tight-Binding single band basis for this problem had the form

$$\varphi_{\mathbf{Q}}^{\sigma_z}(\mathbf{x}, s) = \sqrt{\frac{1}{N}} u^{\sigma_z}(s) \sum_{\mathbf{R}} \exp(i\mathbf{Q} \cdot \mathbf{R}) \varphi_0(\mathbf{x} - \mathbf{R}), \quad (21)$$

where the appearing momenta \mathbf{Q} are given by

$$\mathbf{Q} = \begin{cases} \frac{2\pi}{Lp}(n_{x_1}\mathbf{e}_{x_1} + n_{x_2}\mathbf{e}_{x_2}) \\ n_{x_1}, n_{x_2} \in \mathbb{Z} \\ -\frac{L}{2} \leq n_{x_1}, n_{x_2} < \frac{L}{2} \end{cases}$$

These functions define the Bloch states forming the basis of the maximal translation group with periodic boundary conditions in the same region defined before. In addition $N = L \times L$, and \mathbf{R} are the number of cells in the total lattice of points and the vectors defining the positions of the lattice. Let the HF single particle states expressed in the form

$$\phi_{\mathbf{Q},l}(\mathbf{x}, s) = \sum_{\sigma_z} B_{\sigma_z}^{\mathbf{Q},l} \varphi_{\mathbf{Q}}^{\sigma_z}(\mathbf{x}, s), \quad (22)$$

in the just defined basis. In this case, the equivalent HF matrix problem obtained after substituting these functions in the set of HF equations, is now of dimension two. That is, there are two components $l = 1, 2$ for each momentum \mathbf{Q} . In this way, in an analogous form as in (16) is possible to obtain the HF matrix problem in the form

$$[E_{\mathbf{Q}}^0 + \tilde{\chi}(G_{\mathbf{Q}}^C - G_{\mathbf{Q}}^i - F_{\mathbf{Q}})] \cdot B^{\mathbf{Q},l} = \tilde{\epsilon}_l(\mathbf{Q}) I_{\mathbf{Q}} \cdot B^{\mathbf{Q},l}, \quad (23)$$

which is a system of non linear matrix equations to be solved by iterations.

For starting the iterative process an initial paramagnetic state is employed as an ansatz. The figure 4 shows the doubly degenerated metallic and paramagnetic band which is obtained at half-filling conditions. That is, with $N = 20 \times 20$ electrons. The chosen parameters were: $\epsilon = 12.5$, which is a typical value in semiconductor systems. In what follows we will explain the reasons for selecting the values $\tilde{a} = 0.25$, $\tilde{b} = 0.05$ and $\tilde{\gamma} = 0.03$, always following the criterium of obtaining a band width of $3.8 eV$ as it is suggested by the band diagram in figure 1.

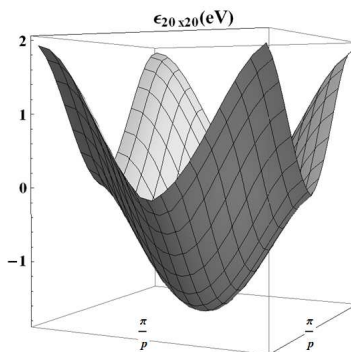


FIG. 4: The doubly degenerated paramagnetic and metallic band arising from the HF solution with full translation symmetry and α and β spin structure of the single particle states.

Observe the coincidence in form between the calculated band and the conduction one appearing in figure 1. In both of them, the Fermi level is crossed by the dispersion curve at the mid point between the top and the bottom of the bands, in the direction Γ - X , while in the direction laying at 45° respect to Γ - X the Fermi level becomes tangent to the dispersion curve in its maximum.

III. EVOLUTION OF THE PARAMAGNETIC-PSEUDOGAP BAND SPECTRUM

In this section we will present the results of solving the HF matrix set of equations for a variable hole doping in the case of the excited solution which evolves from the pseudogap state obtained in Refs. [4–6] for the exact half-filling situation. It is important to recall that this state emerges as a solution after only eliminating the restriction on the single particle states of being a Bloch function in the full lattice formed by all the planar Cu atoms within the CuO_2 planes. The constraints of being single particle states of α or β types were yet maintained. This process allows to obtaining of a doubly degenerated HF solution which shows a pseudogap resembling the one observed in the normal state of the HTc superconductor materials.

Figure 5 shows the evolution with increasing hole concentration of the bands of the pseudogap state, obtained for a point lattice of 20×20 points. All the graphics are plotted in the Brillouin zone of the sublattices, that is the darker zone in the figure 3. Note the existence of a pseudogap which attains its maximum of the order ~ 80 meV. The parameters fixed in the previous section were employed for this evaluation. The maximal value for the gap appears at the mid points of the sides of the Brillouin zone of the sublattices and furnishes an estimate of $T \simeq 1000$ K for the temperature at which the pseudogap starts to be observed in the experiments [12, 13, 20, 21].

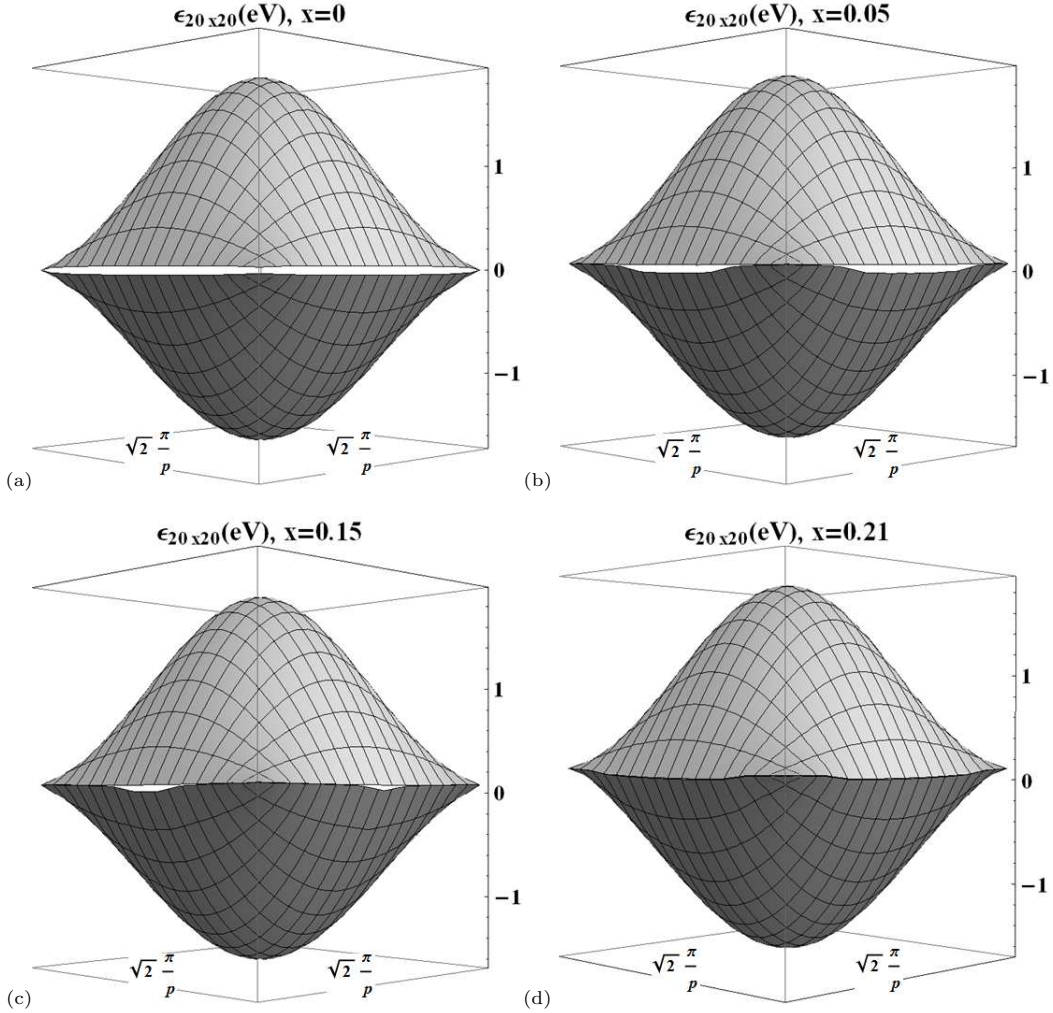


FIG. 5: The evolution of the band spectrum of the PPG as the hole concentration grows. The Fermi level lays in the zero of the graphics. It can be observed how the pseudogap starts closing at the corners of the Brillouin zone as the doping increases.

The evaluated result for the pseudogap depends from the effective dielectric constant ϵ and the set of parameters which were fixed in order to reproduce the single band crossing the Fermi level in the band calculation done by Matheiss [3]. Then, the value obtained here should not be taken as precise prediction for the temperature of the observed pseudogap. However, the ARPES experimental results for the doped La_2CuO_4 indicates a pseudogap

temperature in the region $100-200\text{ meV}$, that is value close to 1000 K . Thus, the *PPG* Hartree-Fock solution offers a reasonable estimate of the pseudogap temperature T^* [12, 13, 20, 21].

One interesting results which can be observed from figure 5 is that by augmenting the hole concentration, the so-called “pockets” [22–24] in the corners of the Brillouin zone are formed. In addition it can be observed that the pseudogap starts to diminish first in the corners until it fully collapses at the critical doping $x_c = 0.2$. After this critical concentration of holes, the state starts behaving as a paramagnetic metal.

IV. EVOLUTION OF THE ANTIFERROMAGNETIC-INSULATOR BAND SPECTRUM

In this section we will consider the solution of the *HF* system of equations (16) by again using the successive iterations method, but in this case, starting from an antiferromagnetic initial ansatz for the Slater determinant state. The results presented below, were found for the values of the set of free parameters: $\epsilon = 12.5$, $\tilde{a} = 0.25$, $\tilde{\gamma} = 0.03$ and $\tilde{b} = 0.05$, which were also employed in the previous section.

The figure 6 (a) shows the band obtained for the point lattice of 20×20 points. The bands are clearly associated to an insulator system, which resulted as the ground state with respect to the pseudogap phase.

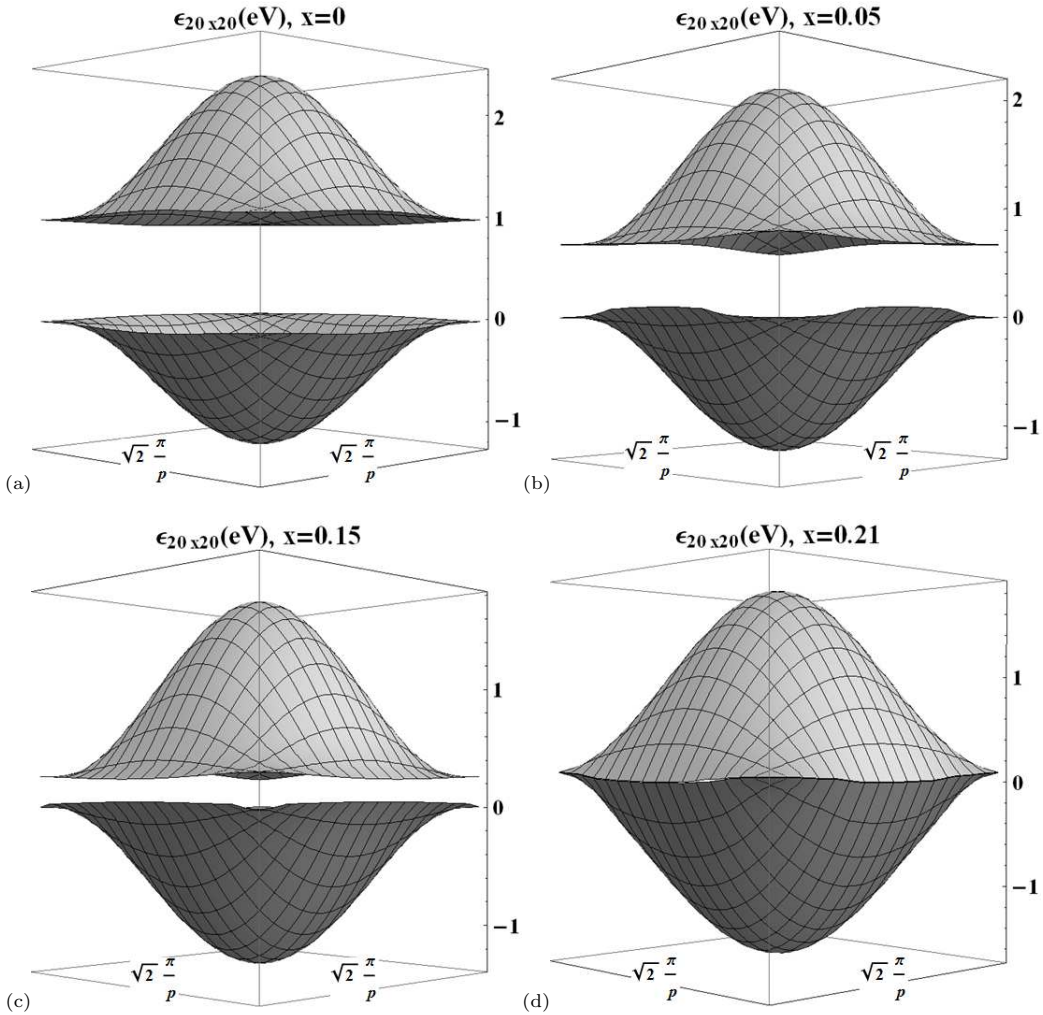


FIG. 6: Evolution of the band spectrum *AFI* as the hole doping increases. The Fermi level is laying in the zero of the plots. The hole states form the the so-called Fermi arcs at the middle of the sides of the reduced Brillouin cell and the gap diminishes until it is fully closed at the critical doping $x_c = 0.2$.

It also shows a local magnetization. These results are essentially the same as the ones obtained in Refs. [4–6] but for slightly different values for the free parameters of the model. The next figures 6 (b), (c), (d) show the evolution

with the increasing hole doping of the band spectrum of these states. It can be observed that the added holes start accumulating at the mid points of the reduced Brillouin zone. That is, in the more energetic electronic states, and as a consequence, more preferable by the holes. All the pictures are plotted in the reduced Brillouin zone of the sublattices. When the doping is further increased up to some critical point, the holes, which were sitting at the mid sides of the Brillouin zone, drastically pass to occupy the corners of the reduced Brillouin zone. This constitute a structural change of the band occurring at the critical value of the hole doping $\delta_c = 0.2$, in which the form of the bands becomes different before and after the states passes through this particular hole concentration. In other words a quantum critical phase transition occurs at this value of the hole doping. Thus, the model predicts a phase transition which had being argued to exist beneath the superconductor dome [10, 11].

The results state that at the moment in which the *AFI* and *PPG* become degenerated at the quantum critical point, the obtained *HF* solution of the problem becomes a unique metallic and paramagnetic phase. An important point to underline, is that, as it is shown in figure 7, around the critical doping $x_c = 0.2$, the results predict that the insulator gap of the *AFI* state diminishes until it completely collapses. The same occurs to the state *PPG*. This produces the metallic behavior which coincides with the one observed in the material in the high doping region.

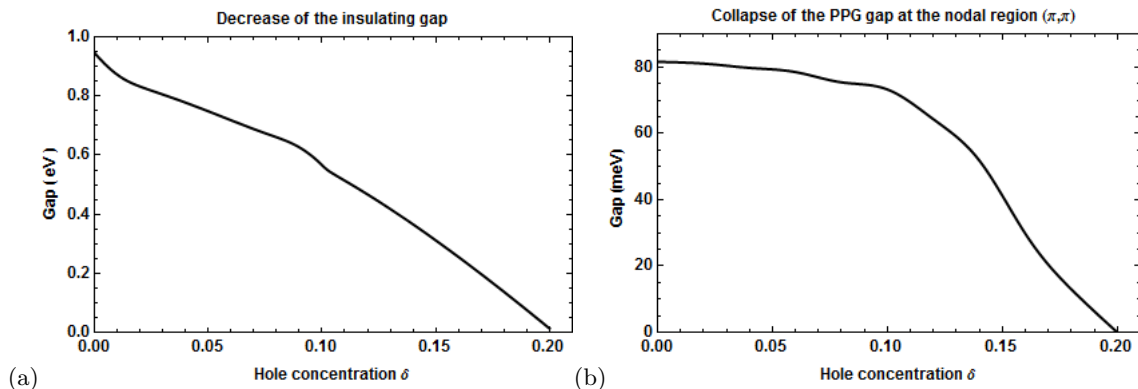


FIG. 7: Diminishing of the gap with the increase of the hole concentration. a) For the antiferromagnetic-insulator spectrum. b) For the paramagnetic-pseudogap state. Note that in both cases the gaps are completely closed when the concentration of holes is $x_c \sim 0.2$, predicting a metallic behavior.

V. EVOLUTION OF THE FERMI SURFACE

Let us expose now the results for the modifications of the Fermi surface induced by the hole doping. The Fermi surface, as separating in the reciprocal space, the occupied from the empty orbitals [25], allows to define many physical properties of the materials. It is known that in the largely non understood normal state of the *HTc* superconductors, the Fermi surface becomes truncated in parts called Fermi arcs. One of the most important open questions in superconductivity theory is how the Fermi arcs and the superconductivity are mutually related [26, 27]. We have investigated the Fermi surface predicted by the model and its dependence on the hole concentration for a wide range of concentrations $0 \leq x \leq 0.3$, defining the evolution with doping from the *AF*-insulator region up to the paramagnetic-metallic one.

The figure 8 shows the evolution of the Fermi surface as the hole doping grows. It can be observed that the model predicts that in the low doping region ($x \leq 0.15$) the Fermi surface is composed of the above mentioned Fermi arcs around the nodal region (π, π) . In this direction is where the doped holes establish as it was mentioned before (the grey zone in figure 8). It was possible to evidence that the length of these arcs grows in proportion with the doping, up to the attainment of the critical doping at $x_c = 0.2$, where a sort of hole pockets form in the corners of the reduced Brillouin zone.

In accordance with our calculations shown in figure 8, the Fermi surface for $x = 0.3$ becomes squared and has a large straight portion around the point $(\frac{\pi}{2}, \frac{\pi}{2})$. The areas closed by the Fermi surfaces are 70, 80, 85 and 95% of the half Brillouin zone area and corresponds to $x = 0.3, 0.2, 0.15$ and 0.05 , respectively. These proportions are consistent with the Luttinger sum rule, if the electron density is $1 - x = (70, 80, 85$ and 95% , respectively). It can be concluded that our results have a close qualitative agreement with the ones shown in figure 9, that were obtained by means of the ARPES in Ref. [9].

Therefore, it follows that the considered model predicts that the Fermi surface of the *LSCO* undergoes a transition, which goes from a hole-like Fermi surface centered at (π, π) for $0 < x < 0.2$ into an electron-like one centered at

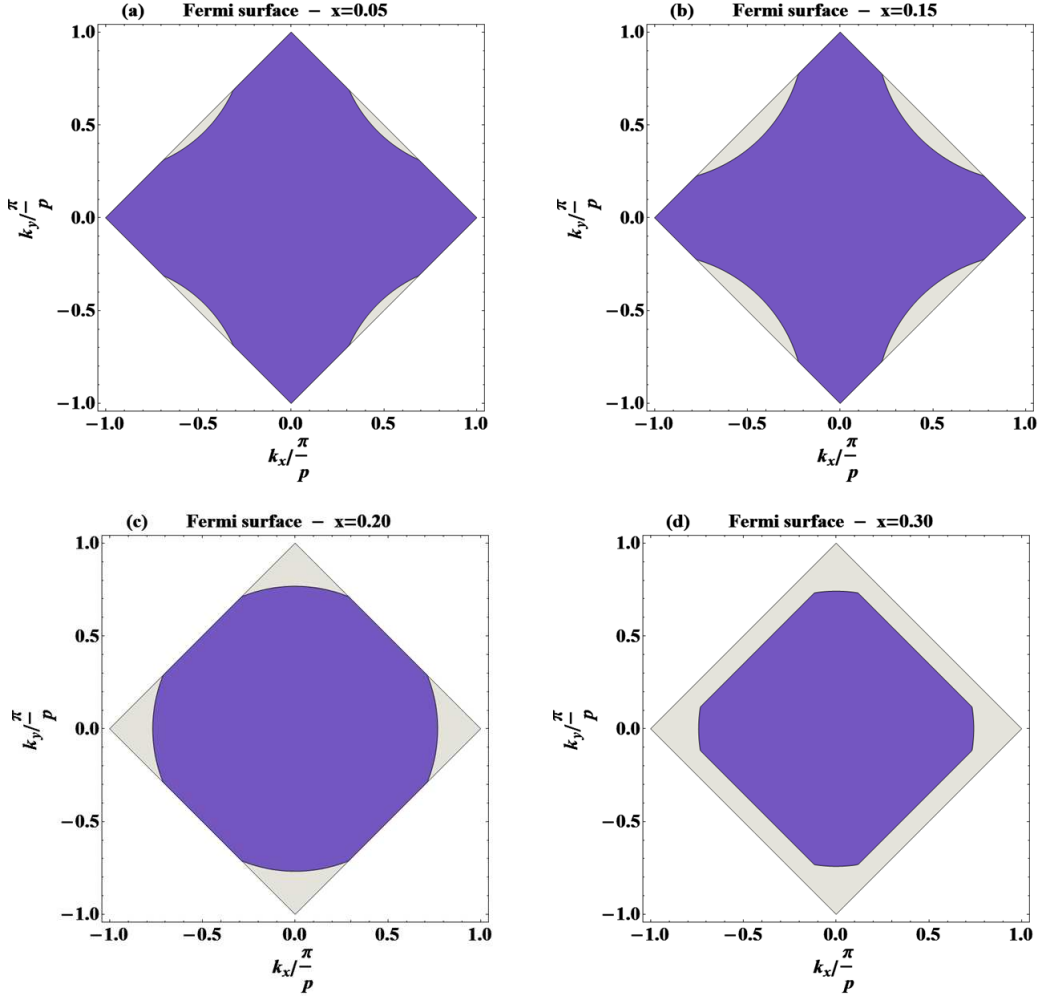


FIG. 8: Evolution of the Fermi surface for increasing hole doping. The areas closed by the Fermi surfaces are 70, 80, 85 and 95% of the half Brillouin zone area and corresponds to $x = 0.3, 0.2, 0.15$ and 0.05 , respectively. These proportions are consistent with the Luttinger sum rule, if the electron density is $1 - x = (70, 80, 85$ and 95% , respectively).

$(0,0)$ for $0.2 < x \leq 0.3$. It is believed that the drastic change of the Fermi surface can correspond with the fact that the sign of the Hall coefficient changes from positive to negative values around $x = 0.25$ in the *LSCO* [28, 29]. In the framework of the investigated model, the mentioned change is associated to the occurrence of a quantum phase transition around the critical point $x_c = 0.2$ which lay beneath the superconductor dome.

VI. THE QUANTUM PHASE TRANSITION

One of the current questions in *HTc* superconductor theory is the occurrence of the superconductivity as determined by the existence of a quantum critical point laying within the hole doping interval at which the superconductivity occurs. Today is widely debated the question about what is the detailed connection between the critical point and the superconductivity effect. Experimental indications about the existence of a critical quantum point comes from the transport and thermodynamic measurements [30–33]. In the framework of the present study, the *HF* energy per particle for the *AFI* and *PPG* states were evaluated by varying the hole concentration in the range $0 \leq x \leq 0.3$, by using the formula

$$E_{\mathbf{k},l}^{HF} = \sum_{\mathbf{k},l} \Theta_{(\tilde{\varepsilon}_F - \tilde{\varepsilon}_l(\mathbf{k}))} [\tilde{\varepsilon}_l(\mathbf{k}) - \frac{\tilde{\chi}}{2} B^{\mathbf{k},l*} \cdot (G_{\mathbf{k}}^C - G_{\mathbf{k}}^i) \cdot B^{\mathbf{k},l}].$$

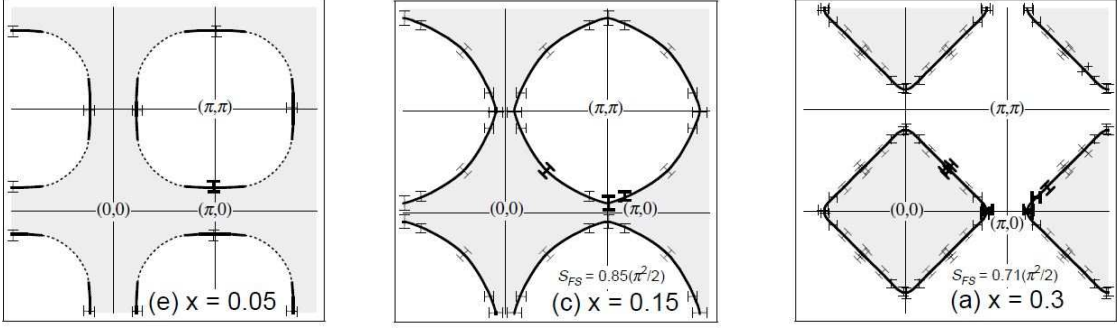


FIG. 9: Evolution of the Fermi surface for increasing hole concentration for the $La_{2-x}Sr_xCuO_4$, obtained by the ARPES experiment. Taken from: Ino A 1999. The dotted line in the first figure represent the so-called Fermi arc. That is a discontinuous Fermi surface.

The figure 10 (a) show how the *AFI* state, which have the lowest energy at half-filling, evolves and becomes degenerate with the *PPG* state at the critical doping $x_c = 0.2$. At this point, as it can be seen in the figure 6, the results predict for the *AFI* state, that the insulator gap diminishes to be completely closed. The same behavior is shown by the *PPG* state for which the momentum dependent pseudogap collapses. The solution of the problem determines a metallic behavior which is the observed nature of La_2CuO_4 for high hole concentrations.

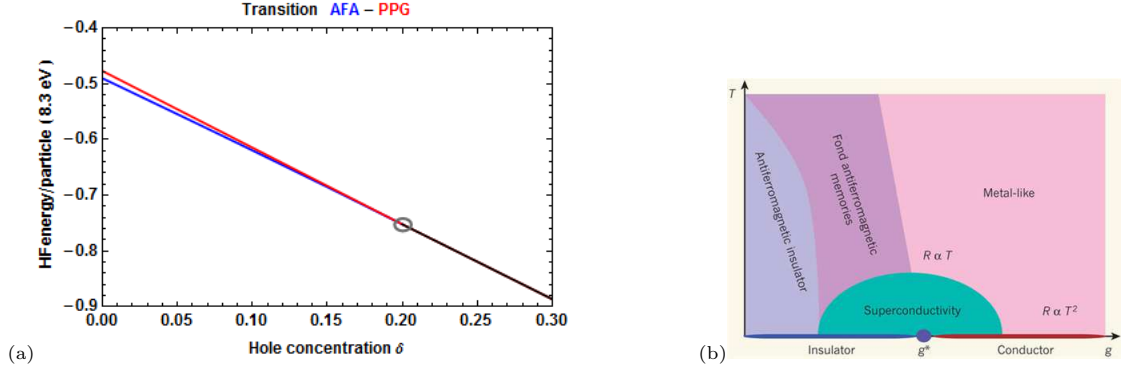


FIG. 10: (a) Dependence of the *HF* energy per particle with the hole doping for the *AFI* and *PPG* states. (b) Generic phase diagram where it can be observed the quantum phase transition from the *AFI* state to a paramagnetic-conductor.

The magnetization of the *AFI* state was also evaluated by its defining formula

$$\mathbf{m}(\mathbf{x}) = \sum_{\mathbf{k}, l} \sum_{s, s'} \phi_{\mathbf{k}, l}^*(\mathbf{x}, s) \boldsymbol{\sigma}(s, s') \phi_{\mathbf{k}, l}(\mathbf{x}, s'), \quad (24)$$

where

$$\boldsymbol{\sigma}(s, s') = \sigma_{x_1}(s, s') \mathbf{e}_{x_1} + \sigma_{x_2}(s, s') \mathbf{e}_{x_2} + \sigma_z(s, s') \mathbf{e}_z, \quad (25)$$

and σ_{x_1} , σ_{x_2} and σ_z are the Pauli matrices. One important conclusion in this study is that in approaching the critical doping value the local magnetization of the *AFI* state tends to vanish (see figure 11), a property that the *PPG* showed along its whole hole doping evolution from the initial half-filled state.

VII. A NEW HOLE BINDING MECHANISM: SPIN-SPACE ENTANGLEMENT

The evaluation procedure of the energy for the *AFI* state in the region of low doping showed a clear dependence on the odd or even character of the number of holes added. That is, it was needed a very much larger number of iterations for attaining convergence when the number of holes was odd.

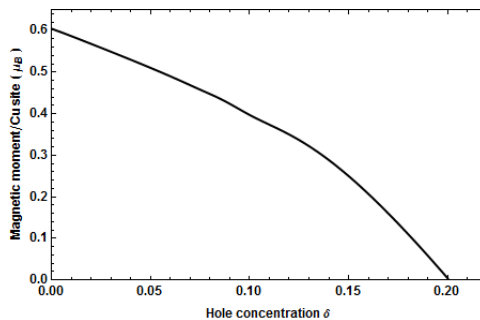


FIG. 11: Reduction of the magnetic moment of the *AFI* state under the doping increasing.

We estimate that a reason for such a behavior might be that adding an odd number of holes, could be expected to show a larger complexity of the *HF* single particle states, since the Kramers degeneracy should be implemented. That is, it could be expected that the double degeneracy implied by the time inversion invariance of the system, when the odd number of holes does not allow to fill an integer number of degenerate pairs of states, should make such single particle states to show a very much complex structure.

A perhaps related circumstance is that the spin-spatial entangled structure of the *HF* single particle states leads to imagine a mechanism of hole pairing that could be acting in the considered system. The idea is that this entangled structure of the single particle states might produce that two, well separated in space, hole wave packets could show, each of them, their relatively complex spin-spatial entangled constitution. However, when the two holes are allowed to be close in space, it is possible that they could tend to compensate their spatially dependent spin and magnetic moment structures and show a lower energy than the other pair of well separated holes. In the case of the paramagnetic systems such an effect seem to be very much weaker, due to the simplicity of the spin structure.

In order to check for this possibility we defined a quantitative measure of the binding between two holes in the antiferromagnetic state. This definition was based in the energy of the ground state of the system E_0 at half-filling and the ground state energies after doped with one hole E_1 and with two holes E_2 in the form

$$\Delta_B = e_2 - 2e_1,$$

where $e_1 = E_1 - E_0$ and $e_2 = E_2 - E_0$. Whenever, two holes minimize their energy by producing a bound state, then Δ_B becomes negative. When Δ_B vanishes the holes may not form a bound state since then $e_2 = 2e_1$ and it is expected that they behave as independent excitations.

The binding energy of two holes Δ_B as a function of the dielectric constant ϵ for point lattices of 16×16 sites (squares) and 20×20 sites (circles) in the case of the *AFI* state is shown in figure 12. Note that the bound states of the two holes form at low doping value as helped by the amount of dielectric screening of the Coulomb interaction. The figure 12 indicates that in general, when the dielectric constant ϵ increases, the binding energy reduces until they form a bound state. The critical value for the appearance of binding for the holes slowly grow with the increasing of the size of the sample (the region in which periodic boundary conditions were imposed).

The results indicate that although the thermodynamical limit is not yet attained for the evaluation of this quantity Δ_B , it seemingly exists. An interesting result is that in La_2CuO_4 , it has experimentally determined that a superconductor gap Δ_{SC} is the order of the $10 meV$ [9], which is of the similar magnitude of the shown values in figure 12, for the two holes binding energy. That is, the measured superconductor gap approximately coincides with the energies Δ_B required to break the two bound holes. This outcome suggests the possibility that the *HF* solution is able to also convey a pairing effect determining the presence of *HTc* superconductivity and the constitution of the Cooper pairs.

A possibly acting binding mechanism could be as follows. Firstly, recall that the *HF* single particle states show the more complicate than the standard spin-spatial entangled structure. This complex composition can be expect to provoke, if the screening is assumed to be strongly enough, a diminishing energy effect, in which the respective entangled magnetic moment structure of the combined two states could tend to compensate one to another. Such an effect should appear in the bound state Bethe-Salpeter equations for two holes. In the described picture, the bound state of two holes at low doping in the *AFI* phase will be formed in this picture thanks to the screening of the Coulomb interaction. The fact that the measured static dielectric constant of the La_2CuO_4 is around the value 25, indicates that the amount of screening is high.

In the more investigated models, like the $t - J$ one, it is argued that the existence of each hole breaks four antiferromagnetic bounds [2], an effect that have an energy cost of the order of the coupling energy ($0.1 eV$). Therefore, at least in the low hole density limit, like the case under consideration, two holes minimize the energy to create them by sharing a common bound. In this way they minimize the number of broken antiferromagnetic bounds. Note that

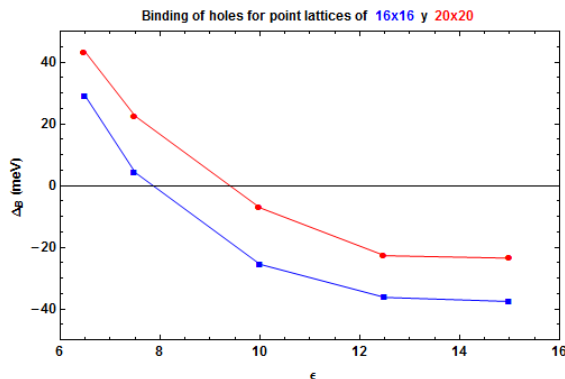


FIG. 12: Binding energy Δ_B of two holes as a function of the dielectric constant ϵ for point lattices of 16×16 (blue squares) and 20×20 (red circles).

this picture seems to be compatible with the one previously exposed on the basis of the spin-spatial entangled nature of the hole states. It is also known that the size of the Cooper pairs of the material is a small quantity (around two lattice constants) [2].

It had been also argued that the existence of preformed hole pairs could not be sufficient evidence for the appearance of the superconductivity. In the context of the present model, it has been argued that for large values the dielectric constant and the presence of spin-spatial entanglement, the pairs could be formed. Then, let us assume that their pair wave function can be formed by superposing products of single particle waves having momenta values close to the centers of the four reduced Brillouin zone sides in figure 6. Then, the amount of the momentum transfer associated to these functions in the Bethe-Salpeter equation could be expected to produce pair wave functions showing sizes of the order of few lattice cells. If such results to be the situation, then, the hole pairs could be expected to condense at $T = 0 K$ giving rise to a Bose condensate of Cooper pairs showing superconductivity. These possibilities will be investigated elsewhere. In ending this section, we also want to express that the results also suggests that the here argued binding effects between two added holes, could constitute a dynamical foundation of the physical meaning of the charge two boson excitations identified in Ref. [16], as being relevant for the description of Hubbard models.

VIII. CONCLUSIONS

We have investigated the model for the La_2CuO_4 defined in Refs. [4–6] applied to the situation in which the material is doped with holes. The main elements of the model were reviewed by fixing its free parameters and solving the Hartree-Fock equations. The evolution with doping of the band spectrum of the antiferromagnetic-insulator state and the metallic-paramagnetic pseudogap one are presented for a wide range of hole concentrations $0 \leq x \leq 0.3$. Around the critical doping density $x_c = 0.2$, the results show that for the *AFI* state, the band spectrum suffers a change in structure of the bands and the insulating band gap diminishes until its complete closing. A similar process also occurs for the *PPG* state where the pseudogap collapses at the same special hole density. Over this critical density the system only shows a single paramagnetic-metallic state. The magnetization of the *AFI* state becomes zero exactly at the critical point. The solutions evidence that the destruction of the antiferromagnetic order is produced by the fact that added holes tend to occupy the states which show a more intense *AF* order: that ones which are closer to the boundary of the reduced Brillouin zone. The results show a drastic change of the nature of the Fermi surface, which goes from a hole-like Fermi surface centered at (π, π) for $0 < x < 0.2$ into an electron-like one centered at $(0, 0)$ for $0.2 < x \leq 0.3$. Henceforth, the whole discussion had shown that the investigated model predicts the existence of a quantum phase transition at critical doping value which is beneath the superconducting dome in La_2CuO_4 . It was also identified a possibility for the pairing of holes which could give rise to the superconductivity and the bounding energy was estimated. The effect seems to be closely linked to the spin-space “entanglement” effect of the *HF* single particle states. Possible connections with the existence of bosonic doubly charged excitations investigated in Ref. [16] were also pointed out.

In ending, let us comment on some possible extensions of the present work. It seems convenient to consider a new parameter for to be fixed in the Hamiltonian of the model. It is related with the effective mass defining the kinetic term of the free part of Hamiltonian. This constant was assumed to be equal to the electron mass in free space, which, possibly, is a somewhat rude choice, since such electrons are assumed to move in the crystalline potential generated by all the other particles, filling the rest of the many bands. This new freedom in the parameters might be relevant

when the spin-orbit effects will be taken into account in order to describe the magnetic anisotropy of the AF order in further discussions. It would be also of help in allowing to more precisely fix the value of the insulator gap of the AFI state which is known to be close to $2 eV$. One important point in this respect is that the dielectric constant ϵ has been measured for La_2CuO_4 . Therefore, it will be needed to fix the free parameters in order to define the observed value of the gap. At this point it can be noticed that electron effective mass will be an influential value which can control the energy scale of the bands and could be phenomenologically fixed to define the $2 eV$ insulator gap. It can be observed from equations (17) and (18).

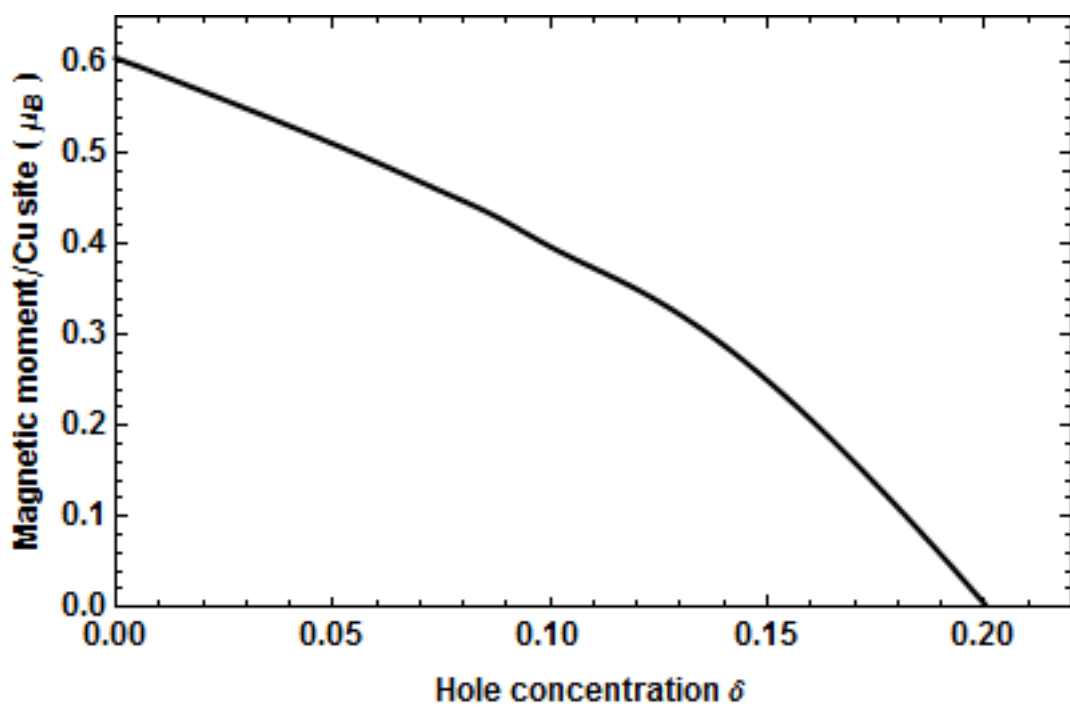
It seems also of interest to perform calculations in order to attain the thermodynamic limit in the hole pairing effect, and also to attempt deriving this binding effect but in the framework of the Bethe-Salpeter equation for two holes moving in the medium. This would confirm the presence of preformed Cooper pairs in the AFI state of the model. Lastly, it will seem convenient to improve the formulation of the model by employing 3D Wannier states resembling the incomplete 3D shell of the Cu atoms within the CuO_2 planes. Upon this, the incorporation of the spin-orbit interactions will be needed in order to further describe the magnetic anisotropy of the AF order in La_2CuO_4 .

Acknowledgments

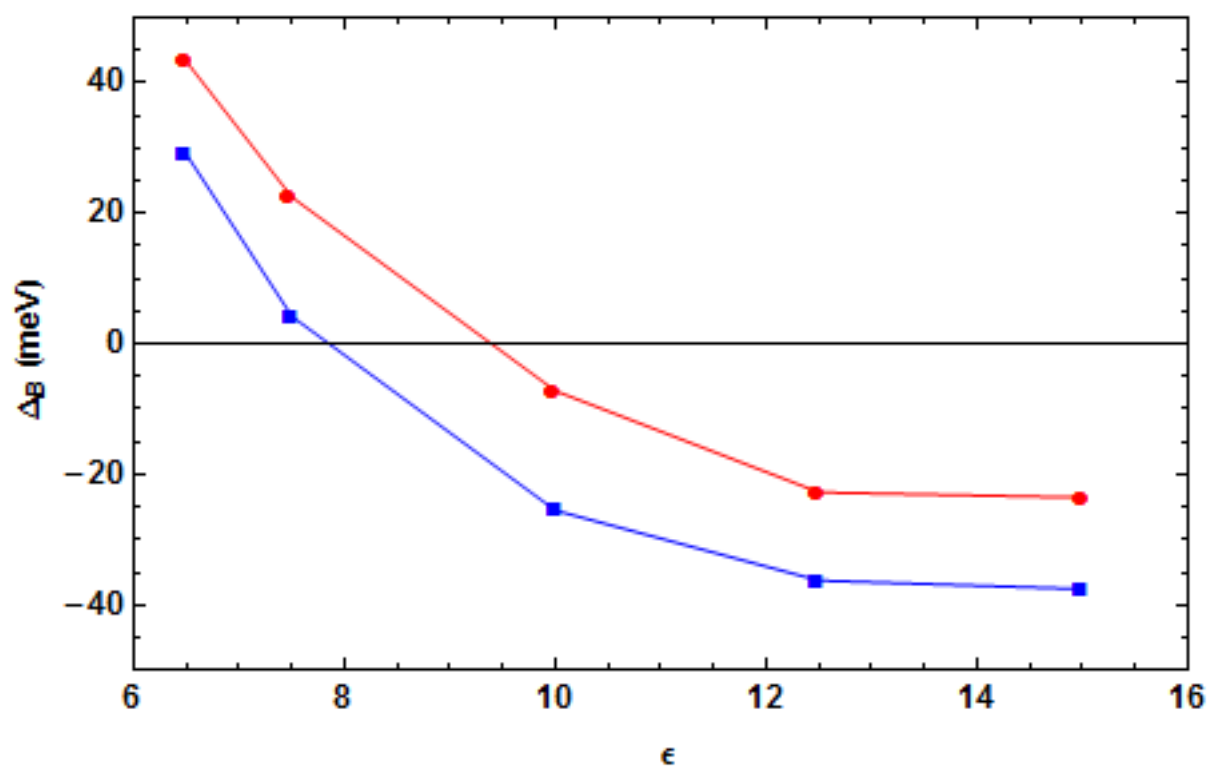
The authors would like to acknowledge the helpful remarks of Profs. E. C. Marino, A. LeClair, A. González, E. Altshuler, A. Odriazola and J. C. Suaáez. We are also indebted by the helpful support received from various institutions: the Caribbean Network on Quantum Mechanics, Particles and Fields (Net-35) of the ICTP Office of External Activities (OEA).

-
- [1] J. G. Bednorz and K. A. Muller, Rev. Mod. Phys. 60, 585 (1987).
 - [2] E. Dagotto, Rev. Mod. Phys. 66, 763 (1994).
 - [3] L. F. Matheiss, Phys. Rev. Lett. 58, 1028 (1987).
 - [4] A. Cabo-Bizet and A. Cabo Montes de Oca, Phys. Lett. A 373, 1865-1869 (2009).
 - [5] A. Cabo-Bizet, A. Cabo Montes de Oca, Symmetry 2, 388 (2010).
 - [6] A. Cabo-Bizet, Una aproximación Hartree Fock al antiferromagnetismo del La_2CuO_4 , Tesis de Diploma, Facultad de Física, Universidad de La Habana (2008).
 - [7] Yen-Sheng Su, T. A. Kaplan, S. D. Mahanti and J. F. Harrison, Phys. Rev. B 59, 10521 (1999).
 - [8] E. Fradkin, Field Theory of Condensed Matter Systems. Addison-Wesley, New York (1991).
 - [9] A. Ino, Photoemission Study of the High-Temperature Superconductor $La_{2-x}Sr_xCuO_4$. Thesis, Department of Physics, University of Tokyo (1999).
 - [10] D. M. Broun, Nature Physics 4, 170 – 172 (2008).
 - [11] S. Sachdev, Physica Status Solidi B 247, 537 – 543 (2010).
 - [12] J. L. Tallon and J. W. Loram, Physica C 349, 53-68 (2001).
 - [13] J.R. Cooper, J.W. Loram, J. Phys. I (France) 6, 2237 (1996).
 - [14] C. Y. Chen, R. J. Birgeneau, M. A. Kastner, N. W. Preyer and Tineke Thio, Phys. Rev. B 43, 392 (1991).
 - [15] J. M. Ginder, M. G. Roe, Y. Song, R. P. McCall, J. R. Gaines, E. Ehrenfreund, and A. J. Epstein, Phys. Rev. B 37, 7506 (1988).
 - [16] R. G. Leigh, P. Phillips and T. P. Choy, Phys. Rev. Lett 99, 046404 (2007).
 - [17] P. A. M. Dirac, Proc. Cambridge. Phil. Soc. 26, 376 (1930).
 - [18] W. E. Pickett, Rev. Mod. Phys. 61, 433 (1989).
 - [19] Y. Yanase, Phys. Rep. 387, 1 (2003).
 - [20] B. Wuyts, V.V. Moshchalkov, Y. Bruynseraede, Phys. Rev. B 53, 9418 (1996).
 - [21] B. Fauqué, Y. Sidis, V. Hinkov, S. Pailh, C. T. Lin., X. Chaud, P. Bourges, Phys. Rev. Lett. 96, 197001 (2006).
 - [22] M. Platé, J. D. F. Mottershead, I. S. Elfimov, D. C. Peets, Ruixing Liang, D. A. Bonn, W. N. Hardy, S. Chiuzbaian, M. Falub, M. Shi, L. Patthey and A. Damascelli, Phys. Rev. Lett. 95, 077001 (2005).
 - [23] K. M. Shen, F. Ronning, D. H. Lu, F. Baumberger, N. J. C. Ingle, W. S. Lee, W. Meevasana, Y. Kohsaka, M. Azuma, M. Takano, H. Takagi and Z.-X. Shen, Science 307, 901-904 (2005).
 - [24] N. Doiron-Leyraud, C. Proust, D. Leboeuf, J. Levallois, J.-B. Bonnemaïson, R. Liang, D. A. Bonn, W. N. Hardy and L. Taillefer, Nature 447, 565-568 (2007).
 - [25] C. Kittel, Introduccion a la Física del Estado Sólido. Editorial Reverté, Barcelona, 3rd Edition (1993).
 - [26] S. Ideta, Electronic Structure and its Relationship to Superconductivity in Iron-based and Cuprate High-Tc Superconductors Studied by Angle-resolved Photoemission Spectroscopy. Thesis, University of Tokyo (2011).
 - [27] S. Ideta, K. Takashima, M. Hashimoto, T. Yoshida, A. Fujimori, H. Anzai, T. Fujita, Y. Nakashima, A. Ino, M. Arita, H. Namatame, M. Taniguchi, K. Ono, M. Kubota, D. H. Lu, Z.-X. Shen, K. M. Kojima and S. Uchida, Phys. Rev. Lett. 104, 227001 (2010).

- [28] K. Tamasaku, T. Ito, H. Takagi and S. Uchida, *Phys. Rev. Lett.* 72, 3088 (1994).
- [29] S. Uchida, H. Takagi, Y. Tokura, N. Koshihara and T. Arima, in: *Strong Correlation and Superconductivity*, edited by H. Fukuyama, S. Maekawa and A. P. Malozemof, Springer-Verlag, Berlin (1989).
- [30] F. F. Balakirev, J. B. Betts, A. Migliori, I. Tsukada, Y. Ando and G. S. Boebinger, *Phys. Rev. Lett.* 102, 017004 (2009).
- [31] R. Daou, N. Doiron-Leyraud, D. LeBoeuf, S. Y. Li, F. Lalibert, O. Cyr-Choinire, Y. J. Jo, L. Balicas, J.-Q. Yan, J.-S. Zhou, J. B. Goodenough and L. Taillefer, *Nat. Phys.* 5, 31-34 (2009).
- [32] D. van der Marel, H. J. A. Molegraaf, J. Zaanen, Z. Nussinov, F. Carbone, A. Damascelli, H. Eisaki, M. Greven, P. H. Kes and M. Li, *Nature* 425, 271 (2003).
- [33] C. Bernhard, J. L. Tallon, T. Blasius, A. Golnik and C. Niedermayer, *Phys. Rev. Lett.* 86, 1614-1617 (2001).



Binding of holes for point lattices of 16x16 y 20x20



Transition AFA - PPG

